PHYSICAL REVIEW D **85,** 115024 (2012)

Higgs boson decays, baryon number violation, and supersymmetry at the LHC

Jonathan M. Arnold
California Institute of Technology, Pasadena, California 91125, USA

Pavel Fileviez Pérez
Center for Cosmology and Particle Physics (CCPP), New York University, 4 Washington Place, New York, New York 10003, USA

Bartosz Fornal
California Institute of Technology, Pasadena, California 91125, USA

Sogee Spinner
International School for Advanced Studies (SISSA), Via Bonomea 265, 34136 Trieste, Italy
(Received 30 April 2012; published 26 June 2012)

Baryon number violating interactions could modify the signatures of supersymmetric models at the Large Hadron Collider. In this article we investigate the predictions for the Higgs mass and the Higgs decays in a simple extension of the minimal supersymmetric standard model where the local baryon and lepton numbers are spontaneously broken at the TeV scale. This theory predicts baryon number violation at the low scale that can change the current LHC bounds on the supersymmetric spectrum. Using the ATLAS and CMS bounds on the Higgs mass we show the constraints on the sfermion masses and show the subsequent predictions for the radiative Higgs decays. We found that the Higgs decay into two photons is suppressed due to the existence of new light leptons. In this theory the stops can be very light in agreement with all experimental bounds, and we make a brief discussion of the possible signals at the LHC.

DOI: 10.1103/PhysRevD.85.115024 PACS numbers: 12.60.Jv, 14.80.Da

I. INTRODUCTION

The minimal supersymmetric extension of the standard model (MSSM) is considered as one of the most appealing theories to describe physics at the TeV scale. While this theory makes many interesting predictions the signals at the Large Hadron Collider (LHC) depend on unknowns such as the supersymmetric spectrum and the presence or absence of baryon (B) and lepton (L) number violating interactions (collectively known as R-parity violating interactions). The CMS [1] and ATLAS [2] experiments have studied many possible signals of the MSSM at the LHC setting very strong bounds on the gluino and squarks masses in some specific scenarios with missing energy. In the majority of the experimental studies it is assumed the absence of the baryon (B) and lepton (L) number violating interactions (R-parity conservation). However, it is well known that in general the B and L symmetries can be broken changing many of the predictions for the collider experiments. For example, one could modify all collider bounds based on the searches for missing energy if the baryon number is broken.

In this article we discuss the possible impact of the baryon number violating interactions on the supersymmetric signals at the LHC. We focus our study in the context of a simple extension of the MSSM where the baryon and lepton numbers are local gauge symmetries spontaneously broken at the TeV scale. We refer to this theory as the "BLMSSM" [3]. The main motivation for this theory is that a large desert between the electroweak scale and grand unified scale is no longer necessary since, while B and L are broken at the low scale the proton remains stable. In the BLMSSM the lepton number is broken in an even number while the baryon number violating operators can change B by one unit. Even though new generations of fermions are required, they do not mix with the SM fermions and therefore do not lead to flavor violation at tree level. Furthermore, they are not associated with Landau poles at the low scale. The light Higgs boson mass can be large without assuming a large stop mass and left-right mixing and one could modify the current LHC bounds on the supersymmetric spectrum due to the presence of the baryon number violating interactions.

We study in great detail the correlation between the Higgs mass and the decay of the Higgs boson into two photons following the new results presented by the ATLAS and CMS collaborations. In this theory the new light leptons appreciably decrease the predictions for the Higgs decay into two gammas. Therefore, confirmation of the two-photon signal at the LHC resulting from Higgs decay would rule out this model. In this theory the stops can be very light in agreement with the Higgs mass and colliders bounds.

This article is organized as follows: In Sec. II we discuss the main features of the BLMSSM. The possible impact of the baryon number violating interactions on the LHC searches are discussed in Sec. III. The predictions for the light CP-even Higgs mass and the constraints on the supersymmetric spectrum are investigated in Sec. IV. In Sec. V the radiative Higgs decays are studied, while the evolution of the gauge and Yukawa couplings are investigated in Sec. VI. In the appendices we include all details needed for the numerical calculations.

II. THE BLMSSM

In this article we study a simple supersymmetric model where the baryon number (B) and lepton number (L) are local gauge symmetries [3]. This model is based on the gauge symmetry

$$G_{\rm BL} = SU(3)_C \bigotimes SU(2)_L \bigotimes U(1)_Y \bigotimes U(1)_B \bigotimes U(1)_L.$$

We refer to this model as the BLMSSM. In this context we have found the following [3]:

(i) The local B and L are spontaneously broken at the TeV scale.
(ii) There are no dangerous operators mediating proton decay.
(iii) The lepton number is broken in an even number while the baryon number violating operators can change B by one unit.
(iv) Anomaly cancellation requires the presence of new families; however, there is no flavor violation at tree level since they do not mix with the SM fermions.
(v) There are no Landau poles at the low scale due to the new families.
(vi) The light Higgs boson mass can be large without assuming a large stop mass and left-right mixing.
(vii) One could modify the current LHC bounds on the supersymmetric spectrum due to the presence of the baryon number violating interactions.

In this model we have the chiral superfields of the MSSM, and in order to cancel the B and L anomalies we need a vectorlike family: $\hat{Q}_4$, $\hat{u}_4^c$, $\hat{d}_4^c$, $\hat{L}_4$, $\hat{e}_4^c$, $\hat{\nu}_4^c$ and $\hat{Q}_5^c$, $\hat{u}_5$, $\hat{d}_5$, $\hat{L}_5^c$, $\hat{e}_5$, $\hat{\nu}_5$. See Table I for the superfields present in the BLMSSM.

Interactions.—The full superpotential of the model is given by

$$\mathcal{W}_{\rm BL} = \mathcal{W}_{\rm MSSM} + \mathcal{W}_{\rm B} + \mathcal{W}_{\rm L} + \mathcal{W}_X + \mathcal{W}_5, \quad (1)$$

where

$$\mathcal{W}_{\rm MSSM} = Y_u \hat{Q}\hat{H}_u\hat{u}^c + Y_d\hat{Q}\hat{H}_d\hat{d}^c + Y_e\hat{L}\hat{H}_d\hat{e}^c + \mu\hat{H}_u\hat{H}_d, \quad (2)$$

is the MSSM superpotential and

$$\mathcal{W}_{\rm B} = \lambda_Q\hat{Q}_4\hat{Q}_5^c\hat{S}_B + \lambda_u\hat{u}_4^c\hat{u}_5\hat{\bar{S}}_B + \lambda_d\hat{d}_4^c\hat{d}_5\hat{\bar{S}}_B + \mu_B\hat{\bar{S}}_B\hat{S}_B + Y_{u_4}\hat{Q}_4\hat{H}_u\hat{u}_4^c + Y_{d_4}\hat{Q}_4\hat{H}_d\hat{d}_4^c + Y_{u_5}\hat{Q}_5^c\hat{H}_d\hat{u}_5 + Y_{d_5}\hat{Q}_5^c\hat{H}_u\hat{d}_5. \quad (3)$$

The new quark superfields acquire TeV scale masses once the S_B and $\bar{S}_B$ Higgs fields acquire a vacuum expectation value (VEV). Consequently, the Yukawa couplings of the new quarks to the Higgs fields do not contribute greatly to the new quark masses and can be neglected. Furthermore the Yukawa couplings between the new quarks and the MSSM Higgs bosons can be large and modify the Higgs mass at one-loop level. Notice that these couplings can have a large impact on the production cross section, $gg \to h$, making it difficult to satisfy the experimental bounds on Higgs production. In this work, we will take the conservative approach and assume these new quark Yukawa couplings are small. The Higgs mass is therefore only substantially modified by the Yukawa couplings of the new leptons which must be large to insure the new leptons masses are large enough to satisfy collider bounds.

In the leptonic sector one has the following interactions:

$$\mathcal{W}_{\rm L} = Y_{e_4}\hat{L}_4\hat{H}_d\hat{e}_4^c + Y_{e_5}\hat{L}_5^c\hat{H}_u\hat{e}_5 + Y_{\nu_4}\hat{L}_4\hat{H}_u\hat{\nu}_4^c + Y_{\nu_5}\hat{L}_5^c\hat{H}_d\hat{\nu}_5 + Y_\nu\hat{L}\hat{H}_u\hat{\nu}^c + \lambda_{\nu^c}\hat{\nu}^c\hat{\nu}^c\hat{\bar{S}}_L + \mu_L\hat{\bar{S}}_L\hat{S}_L. \quad (4)$$

Notice that we have an implementation of the seesaw mechanism for the light neutrino masses once the $\bar{S}_L$ field acquires a VEV, while the new neutrinos have Dirac mass terms. In order to avoid stability for the new quarks we add the fields, $\hat{X}$ and $\hat{\bar{X}}$, which have the following interactions:

$$\mathcal{W}_{\rm X} = \lambda_1\hat{Q}\hat{Q}_5^c\hat{X} + \lambda_2\hat{u}^c\hat{u}_5\hat{\bar{X}} + \lambda_3\hat{d}^c\hat{d}_5\hat{\bar{X}} + \mu_X\hat{\bar{X}}\hat{X}, \quad (5)$$

where the baryon number for the new fields are $B_X = 2/3 + B_4 = -B_{\bar{X}}$, and if we assume that they do not get a VEV the lightest one can be a dark matter candidate even if R-parity is violated. See Refs. [4,5] for the use of this idea in a previous version of the model.

For any value of the baryonic charges of the new fermions, which satisfy the anomaly conditions, the Higgses $\hat{S}_B$ and $\hat{\bar{S}}_B$ have charges 1 and -1, respectively. Then, one can write the following dimension five operator that gives rise to baryon number violation once the baryon number is broken through the VEV of S_B:

$$\mathcal{W}_5 = \frac{a_1}{\Lambda}\hat{u}^c\hat{d}^c\hat{d}^c\hat{S}_B. \quad (6)$$

Therefore, after breaking $U(1)_B$ we find the so-called λ'' MSSM interactions that can modify the current LHC bounds on the supersymmetric mass spectrum. Regardless of this R-parity breaking term, the field $X(\bar{X})$ or their superpartners can be a dark matter candidate. The study of the properties of the dark matter candidates is beyond the scope of this article.

A. B and L symmetry breaking

In this section we discuss how the local B and L symmetries are broken. In this context the local gauge group, $G_{\rm BL}$, is broken to $G_{\rm SM} \bigotimes M_L$. Here $G_{\rm SM}$ is the SM gauge group and $M_L = (-1)^L$ is the lepton parity:

$$G_{\rm BL} \longrightarrow G_{\rm SM} \bigotimes M_L.$$

In this model the local baryonic symmetry $U(1)_B$ is broken by the VEV of the scalar fields $S_B \sim (1, 1, 0, 1, 0)$ and $\bar{S}_B \sim (1, 1, 0, -1, 0)$. The relevant scalar potential is given by

$$V_B = \frac{g_B^2}{8}(|S_B|^2 - |\bar{S}_B|^2)^2 + (|\mu_B|^2 + m_{S_B}^2)|S_B|^2 + (|\mu_B|^2 + m_{\bar{S}_B}^2)|\bar{S}_B|^2 - (b_B S_B \bar{S}_B + \text{H.c.}). \quad (7)$$

Defining the VEVs, $\langle S_B \rangle = v_B/\sqrt{2}$ and $\langle \bar{S}_B \rangle = \bar{v}_B/\sqrt{2}$, the minimization conditions read as

$$|\mu_B|^2 + m_{S_B}^2 + \tfrac{1}{2}M_{Z_B}^2 \cos2\beta_B - b_B \tan\beta_B = 0, \quad (8)$$

$$|\mu_B|^2 + m_{\bar{S}_B}^2 - \tfrac{1}{2}M_{Z_B}^2 \cos2\beta_B - b_B \cot\beta_B = 0, \quad (9)$$

where $\tan\beta_B = \bar{v}_B/v_B$ and $M_{Z_B}^2 = g_B^2(v_B^2 + \bar{v}_B^2)/4$. Assuming that the potential is bounded from below along the D-flat direction one finds the condition

$$2b_B < 2|\mu_B|^2 + m_{S_B}^2 + m_{\bar{S}_B}^2, \quad (10)$$

while

$$b_B^2 > (|\mu_B|^2 + m_{S_B}^2)(|\mu_B|^2 + m_{\bar{S}_B}^2), \quad (11)$$

in order to have a nontrivial minimum. It is important to emphasize that the symmetry $U(1)_B$ is broken at the TeV scale, and therefore the mass of the new neutral gauge boson is related to the SUSY breaking mass scale. In order to show this we give the dependence of the new gauge boson masses on the parameters in the model:

$$\frac{1}{2}M_{Z_B}^2 = -|\mu_B|^2 + \left(\frac{m_{S_B}^2 - m_{\bar{S}_B}^2 \tan^2\beta_B}{\tan^2\beta_B - 1}\right). \quad (12)$$

We note here that the experimental bounds on leptophobic gauge bosons with masses below the TeV scale are very weak due to QCD backgrounds. The most relevant bound, $M_{Z_B} > 250$ GeV, comes from the UA2 experiment assuming SM-like couplings [6]. For higher masses, the CMS Collaboration has placed bounds on new resonances decaying into $t\bar{t}$ pairs [7]. In this case, the resonance must have a mass of more than 1 TeV.

Once B is broken we can find new interactions that violate baryon number. Using Eq. (6) one finds

$$2\lambda''_{ijk} u_i^c d_j^c \tilde{d}_k^c \quad \text{and} \quad \lambda''_{ijk} \tilde{u}_i^c d_j^c d_k^c, \quad (13)$$

with

$$\lambda''_{ijk} = a_1^{ijk} \frac{v_B}{\Lambda\sqrt{2}}, \quad (14)$$

where $a_1^{ijk} = -a_1^{ikj}$. These interactions break baryon number in one unit and are the so-called λ''_{ijk} terms of the MSSM.

As in the case of the baryon number the local $U(1)_L$ is broken at the TeV scale by the VEV of the scalar fields S_L and $\bar{S}_L$. Following the discussion above one can find a similar relation between the quark-phobic gauge boson mass and the soft terms of the scalar fields:

$$\frac{1}{2}M_{Z_L}^2 = -|\mu_L|^2 + \left(\frac{m_{S_L}^2 - m_{\bar{S}_L}^2 \tan^2\beta_L}{\tan^2\beta_L - 1}\right). \quad (15)$$

The strongest bounds on quark-phobic gauge bosons come from LEP2, which found a lower mass bound of 1.8 TeV [8]. In the above equations $m_{S_L}(m_{S_B})$ and $m_{\bar{S}_L}(m_{\bar{S}_B})$ are soft masses for the Higgses $S_L(S_B)$ and $\bar{S}_L(\bar{S}_B)$, while $\tan\beta_L = \langle \bar{S}_L \rangle / \langle S_L \rangle = \bar{v}_L/v_L$ and $M_{Z_L}^2 = g_L^2(v_L^2 + \bar{v}_L^2)$.

Now, after symmetry breaking one can see that the lepton number is only broken in two units. Using the term, $\hat{\nu}^c \hat{\nu}^c \hat{\bar{S}}_L$, in Eq. (4) one finds the Majorana mass term for the right-handed neutrinos

$$\lambda_{\nu^c}^{ij} \nu_i^c \nu_j^c \frac{\bar{v}_L}{\sqrt{2}}, \quad (16)$$

which is needed to generate neutrino masses through the seesaw mechanism.

Summarizing, in this model the local B and L symmetries can be broken at the TeV scale while contributions to proton decay are not induced because the baryon number is broken by one unit and the lepton number is broken by two units as required by the seesaw mechanism. There are relevant constraints coming from the $\Delta B = 2$ processes, such as $n - \bar{n}$ oscillations and dinucleon decays, and from cosmology which we will discuss in the next sections.

B. Mass spectrum

New leptons.—The mass for the new leptons are given by

$$M_{e_4} = Y_{e_4}\frac{v_d}{\sqrt{2}}, \qquad M_{e_5} = Y_{e_5}\frac{v_u}{\sqrt{2}}, \qquad M_{\nu_4} = Y_{\nu_4}\frac{v_u}{\sqrt{2}}, \quad \text{and} \quad M_{\nu_5} = Y_{\nu_5}\frac{v_d}{\sqrt{2}}. \quad (17)$$

Using the above equations and imposing the perturbative condition for the Yukawa coupling, $Y_{e_4}^2/4\pi \leq 1$, one finds an upper bound on $\tan\beta$:

$$\tan\beta \leq 6.1(4.3),$$

when $M_{e_4} \geq 100(140)$ GeV.

Sfermion masses.—In this model the sfermion masses are modified due to existence of new D terms. For example, the stop mass matrix reads as

$$\begin{pmatrix} M_t^2 + M_{\tilde{Q}_3}^2 + \left(\frac{1}{2} - \frac{2}{3}\sin^2\theta_W\right) M_Z^2 \cos 2\beta + \frac{1}{3} D_B & M_t X_t \\ M_t X_t & M_t^2 + M_{\tilde{u}_3^c}^2 + \frac{2}{3}\sin^2\theta_W M_Z^2 \cos 2\beta - \frac{1}{3} D_B \end{pmatrix}, \tag{18}$$

where $M_{\tilde{Q}_3}^2$ and $M_{\tilde{u}_3^c}^2$ are squark soft masses. $D_B = \frac{1}{2} M_{Z_B}^2 \cos 2\beta_B$ defines the new contribution due to the presence of the $U(1)_B$ D term, M_t is the top mass, and $X_t = A_t - \mu \cot\beta$ is the left-right mixing in the stop sector. In a similar way we can write the mass matrix for the sbottoms. See Appendix B for details.

The new slepton mass is modified by the $U(1)_L$ D term. The mass matrix for the fifth generation sleptons reads as

$$\mathcal{M}_{\tilde{\nu}_5}^2 = \begin{pmatrix} M_{\nu_5}^2 + M_{\tilde{L}_5^c}^2 - \frac{1}{2} M_Z^2 \cos 2\beta - (3 + L_4) D_L & M_{\nu_5} X_{\nu_5} \\ M_{\nu_5} X_{\nu_5} & M_{\nu_5}^2 + M_{\tilde{\nu}_5}^2 + (3 + L_4) D_L \end{pmatrix}. \tag{19}$$

Here $D_L = -\frac{1}{4} M_{Z_L}^2 \cos 2\beta_L$ is the new D term contribution and $X_{\nu_5} = A_{\nu_5} - \mu \tan\beta$ the left-right mixing in this sector. In order to simplify the discussion in the text we list the mass matrices for the other sfermions in the Appendix.

III. BARYON NUMBER VIOLATION AND THE SUSY SPECTRUM

When the baryon asymmetry is generated above the electroweak scale strong bounds on the $\lambda''_{ijk} u_i^c d_j^c d_k^c$ couplings exist from the condition that the $2 \to 2$ and $2 \to 1$ processes do not wash out the baryon asymmetry generated. These constraints have been studied in great details in Refs. [9–12]. The bound on these couplings read as [10,12]

$$\lambda''_{ijk} \lesssim 5 \times 10^{-7} \left(\frac{M_{\tilde{q}}}{1\ \mathrm{TeV}}\right)^{1/2}, \tag{20}$$

where $M_{\tilde{q}}$ is the squark mass. Now, in order to understand the impact of this bound on the SUSY signals we will consider different scenarios for the lightest supersymmetric particle (LSP):

(i) *Neutralino as the LSP.*—In this case the neutralino will decay into three quarks and one can have the following signals:

$$pp \to \tilde{t}^* \tilde{t} \to \bar{t} t \tilde{\chi}_1^0 \tilde{\chi}_1^0 \to \bar{t} t 6j,$$
$$pp \to \tilde{b}^* \tilde{b} \to \bar{b} b \tilde{\chi}_1^0 \tilde{\chi}_1^0 \to \bar{b} b 6j.$$

Therefore, one could modify the bounds on the supersymmetric spectra since there is no missing energy in these channels. The neutralino decay length can naively be estimated as

$$\mathrm{L}(\tilde{\chi}^0 \to 3q) > 160\ \mathrm{m} \left(\frac{M_{\tilde{q}}}{500\ \mathrm{GeV}}\right)^4 \left(\frac{100\ \mathrm{GeV}}{M_{\tilde{\chi}^0}}\right)^5 \times \left(\frac{2.5 \times 10^{-7}}{\lambda''}\right)^2, \tag{21}$$

assuming the cosmological bounds. Therefore, the lightest neutralino would decay outside the detector and one has the standard signals with missing energy at the LHC. However, if the baryogenesis mechanism is at the weak scale one can avoid the bounds from cosmology and the neutralino can decay inside the detector.

(ii) *Gluino as the LSP.*—In this case the gluino pair production can lead to channels with same-sign tops and multijets

$$pp \to \tilde{g}\,\tilde{g} \to tt4j,\ bb4j.$$

Now, assuming the constraint coming from cosmology, one can estimate naively the decay length of the gluino as

$$\mathrm{L}(\tilde{g} \to 3q) > 10\ \mathrm{m} \left(\frac{M_{\tilde{q}}}{10^3\ \mathrm{GeV}}\right)^4 \left(\frac{400\ \mathrm{GeV}}{M_{\tilde{g}}}\right)^5 \times \left(\frac{10^{-7}}{\lambda''}\right)^2. \tag{22}$$

Therefore, the gluino is long-lived and forms bounded states. The resulting states that consist of either of a gluino pair or triplets of quarks, or of a gluino bound to a gluon, are called R-hadrons [13]. If the gluinos are produced near threshold, the formation of gluino-pair bound states (gluinonium) is also possible and leads to characteristic signals [14–18] and places strong bounds on the gluino mass.

(iii) *Slepton as the LSP.*—If the LSP is a charged selectron one has a long-lived charged track since the decay length is very large due to the bound coming from cosmology and the four-body phase space suppression. This scenario is very similar to the long-lived stau scenario in gauge mediation [19,20] and one can have signals with two leptons, a same-sign top pair and four jets

$$pp \to \tilde{e}_i^* \tilde{e}_i \to e_i^+ e_i^- tt4j,\ e_i^+ e_i^- bb4j.$$

In the case when the sneutrino is the LSP, one has missing energy and multijets

$$pp \to \tilde{\nu}_i^* \tilde{\nu}_i \to \bar{\nu}\nu tt4j,\ \bar{\nu}\nu bb4j.$$

This scenario is possible and will have constraints from the missing energy searches.

(iv) *Chargino as the LSP.*—The case of a long-lived chargino is very similar to the previous scenario where one has a long-lived charged slepton. One has charged tracks due to existence of a long-lived charged particle and we can have the following signals:

$$pp \to \tilde{\chi}_i^+ \tilde{\chi}_i^- \to W^+ W^- tt4j,\, W^+ W^- bb4j,$$

with same-sign top pair and multijets.

(v) *Squark as the LSP.*—:Because of the cosmological constraint, the squarks will be long-lived and form bounded states. If we compute the decay length of an squark, one finds

$$\mathrm{L}\,(\tilde{q}_i \to q_j q_k) > 1\ \mathrm{mm}\left(\frac{10^2\ \mathrm{GeV}}{M_{\tilde{q}}}\right)\left(\frac{10^{-7}}{\lambda''}\right)^2. \quad (23)$$

Therefore, the squark will form bounded states but it will decay inside the detector. In this case we can have displaced vertices as well when the stop (sbottom) has mass around 100 GeV, and we can have signals with four jets

$$pp \to \tilde{t}^* \tilde{t} \to 4j,\; pp \to \tilde{b}^* \tilde{b} \to 4j.$$

Therefore, one can avoid the LHC constraints coming from the searches for multijets and missing energy. Notice that this scenario is quite relevant for us because we will study different cases where the stop is quite light. It is important to mention that in the model discussed in this article the above constraints are relevant even if the baryon number is broken at the TeV scale. In general one can have an asymmetry in the SM sector and in the dark matter sector, where we have the X field. In this case, the baryon asymmetry can be generated after the breaking of $U(1)_B$. Although it is beyond the scope of this article, a detailed investigation of baryogenesis has been performed for similar models [5]. Now, we have discussed above that the $u^c d^c d^c$ interactions are generated at the TeV scale, and if they are in thermal equilibrium before the electroweak phase transition, around 100 GeV, one cannot preserve the baryon asymmetry in the visible sector. Therefore, in order to make sure that the asymmetry in the visible sector is not washed out, we impose the above constraints.

It is well known that if the baryon asymmetry is generated below the electroweak scale, the bounds on λ''_{ijk} listed above are not present. However, there are other bounds on these couplings. The most important coming from dinucleon decay, $pp \to K^+ K^-$ [21], and one gets $\lambda''_{uds} < 10^{-8}$ [22]. If we use this bound and the one above from cosmology, we can impose a lower bound on the cutoff of the theory. Using $\lambda'' < 10^{-8}$, $\langle S_B \rangle \sim 1$ TeV, and $a_1 \sim 1$, one gets

$$\frac{a_1}{\Lambda}\langle S_B \rangle < 10^{-8} \longrightarrow \Lambda > 10^{11}\ \mathrm{GeV}. \quad (24)$$

This is the naive lower bound on the cutoff of the theory. Of course, the coupling a_1 can be smaller and the cutoff of the theory can be much lower. In the last section we will use the running of the Yukawa couplings to set the possible cutoff assuming perturbativity at the high scale.

IV. THE LIGHT *CP*-EVEN HIGGS MASS

Recently, the ATLAS Collaboration has published a new combined analysis [23,24] that excludes a SM Higgs boson with mass in the ranges 112.9 –115.5 GeV, 131 –238 GeV, and 251 –466 GeV, while the CMS Collaboration excludes a SM Higgs boson with mass in the range 127.5 –600 GeV [25–27]. Also, it is well known that both collaborations have observed an excess around 125 GeV.

In this article we will consider a conservative scenario where the light *CP*-even Higgs boson is SM-like with mass in the range 115–128 GeV, and using this range we will show the possible constraints on the supersymmetric spectra in the MSSM and in the BLMSSM. In this way we can compare both models and predictions for the radiative Higgs decays showing the possibility of ruling out the BLMMSM if the excess around 125 GeV is confirmed in the new analysis by the ATLAS and CMS Collaborations.

In order to set our notation we define the neutral Higgs bosons as

$$H_u^0 = \frac{1}{\sqrt{2}}(v_u + h_u) + \frac{i}{\sqrt{2}}A_u, \quad (25)$$

and

$$H_d^0 = \frac{1}{\sqrt{2}}(v_d + h_d) + \frac{i}{\sqrt{2}}A_d. \quad (26)$$

Using this notation and working in the basis (h_d, h_u) the mass matrix for the MSSM neutral *CP*-even Higgs is given by

$$\mathcal{M}^2_{\mathrm{even}} = \begin{pmatrix} \mathcal{M}^2_{11} + \Delta_{11} & \mathcal{M}^2_{12} + \Delta_{12} \\ \mathcal{M}^2_{12} + \Delta_{12} & \mathcal{M}^2_{22} + \Delta_{22} \end{pmatrix}, \quad (27)$$

with

$$\mathcal{M}^2_{11} = M_Z^2 \cos^2\beta + M_A^2 \sin^2\beta, \quad (28)$$

$$\mathcal{M}^2_{12} = -(M_A^2 + M_Z^2)\sin\beta\cos\beta, \quad (29)$$

$$\mathcal{M}^2_{22} = M_Z^2 \sin^2\beta + M_A^2 \cos^2\beta, \quad (30)$$

where M_A is the pseudoscalar Higgs mass and $\tan\beta = v_u/v_d$. In order to make the numerical calculations we use FeynHiggs [28] to compute the Higgs mass at a two-loop level and include the one-loop corrections due to the existence of new leptons. These new one-loop corrections were considered in Ref. [29], where it has been shown that one can increase the Higgs mass in more than 5–10 GeV in a large fraction of the parameter space. In this article we go beyond this study and show the general constraints on the supersymmetric spectra if we satisfy the experimental constraints on the Higgs mass.

As we have mentioned above, since we cannot predict the Higgs mass in general, we can use the recent results from ATLAS [23,24] and CMS [25,26] to constrain the allowed parameters in the theory. In order to understand these constraints we will work in the decoupling limit in the Higgs sector, $M_A^2 \gg M_Z^2$, which has the largest contribution at tree level to the Higgs mass in the MSSM, and define some simple scenarios:

(i) *Scenario I:* $X_t = X_b = 0$.—In this case we neglect the left-right mixing in the squark sector and take into account only the contributions of the third generation of quark and squarks in showing the allowed parameter space consistent with a Higgs mass in the range 115 GeV $\leq \mathrm{M_h} \leq$ 128 GeV; we scan over the ranges

$$200\ \mathrm{GeV} \leq M_{\tilde{Q}_3}, M_{\tilde{u}_3^c}, M_{\tilde{d}_3^c} \leq 2\ \mathrm{TeV},$$

$$M_{\nu_4} = M_{\nu_5} = 90\ \mathrm{GeV} \quad \text{and} \quad M_{e_4} = M_{e_5} = 100\ \mathrm{GeV},$$

$$0\ \mathrm{GeV} \leq M_{\tilde{L}_4}, M_{\tilde{e}_4^c}, M_{\tilde{\nu}_4^c}, M_{\tilde{L}_5^c}, M_{\tilde{e}_5}, M_{\tilde{\nu}_5} \leq 1\ \mathrm{TeV},$$

$$M_{Z_B} = M_{Z_L} = 1\mathrm{TeV}, \tan\beta_\mathrm{B} = \tan\beta_\mathrm{L} = 2, \mathrm{L}_4 = -\frac{3}{2},$$

and

$$100\ \mathrm{GeV} \leq M_2 \leq 300\ \mathrm{GeV},$$

$$-300\ \mathrm{GeV} \leq \mu \leq 300\ \mathrm{GeV},$$

$$2 \leq \tan\beta \leq 6, \qquad M_A = 1\ \mathrm{TeV},$$

and show the results making the calculation for the Higgs mass at two-loop level in the MSSM and include the new one-loop corrections in the BLMSSM. We also note that the soft mass parameters of the new sleptons can be as low as zero since they must be at least as massive as the new leptons in this case, which is consistent with experimental bounds.

(ii) *Scenario II:* $X_t \neq 0$ and $X_b \neq 0$.—In the second scenario we take into account the left-right mixing in the stop and sbottom sectors, using the same range for the input parameters as in the previous scenario and

$$-4\ \mathrm{TeV} \leq X_\mathrm{t} \leq 4\ \mathrm{TeV},$$

$$-4\ \mathrm{TeV} \leq X_\mathrm{b} \leq 4\ \mathrm{TeV},$$

for the values of the left-right mixing in the squark sector.

In Fig. 1 we show the allowed parameter space in the MSSM and BLMSSM when the Higgs mass is in the range mentioned above. In the MSSM we compute the Higgs mass at the two-loop level using FeynHiggs and in the BLMSSM we have the extra leptonic one-loop contributions. Notice that the red points correspond to the range when the Higgs mass is between 115 and 122 GeV, while the blue points correspond to the range, 122 GeV $\leq M_h \leq$ 128 GeV. We use $M_{\tilde{g}} = 1$ TeV as the gluino mass. The first main difference to notice is that in the MSSM there is no solution when $X_t = 0$, while this is not the case in the BLMSSM. Therefore, for SUSY breaking scenarios such as gauge mediation where the trilinear terms are small, one can say that in the context of the BLMSSM it is possible to satisfy the bounds on the Higgs mass.

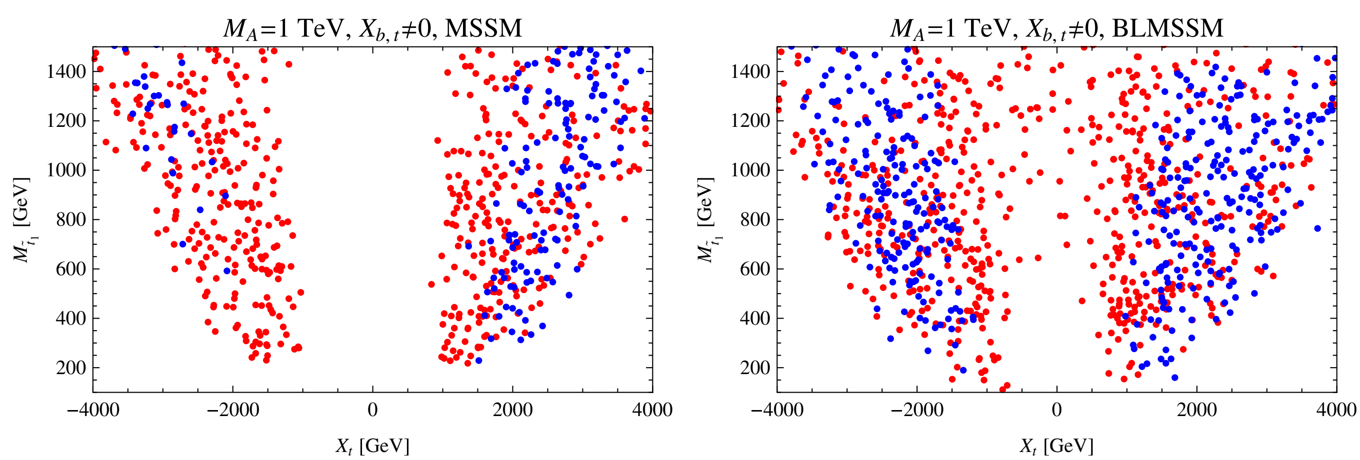

FIG. 1 (color online). Allowed parameter space in the MSSM and BLMSSM in the plane of lightest stop mass versus the left-right mixing in the stop sector. We use as input parameters $M_{\nu_4} = M_{\nu_5} = 90$ GeV and $M_{e_4} = M_{e_5} = 100$ GeV. In the MSSM we compute the Higgs mass at two-loops and in the BLMSSM we have the extra one-loop contributions. The red points correspond to the range when the Higgs mass is between 115 and 122 GeV, while the blue points correspond to the range, 122 GeV $\leq M_h \leq$ 128 GeV. We use $M_{\tilde{g}} = 1$ TeV as the gluino mass. We have checked that all solutions are consistent with the bounds from the absence of color and electric charge breaking.

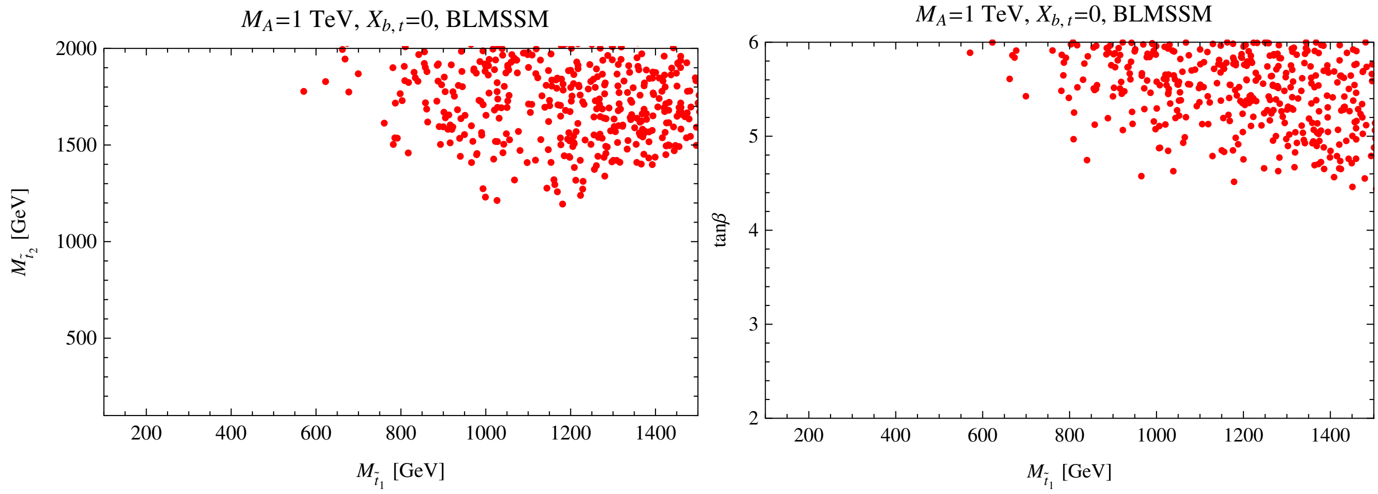

FIG. 2 (color online). Allowed parameter space in the BLMSSM in zero mixing scenario $X_t = X_b = 0$. We use as input parameters $M_{\nu_4} = M_{\nu_5} = 90$ GeV and $M_{e_4} = M_{e_5} = 100$ GeV.

In Fig. 2 we show the allowed parameter space in scenario I for the BLMSSM. Notice that in this case the lightest stop can be as light as 600 GeV, while the heaviest stop is always above 1 TeV. For our input parameters we find allowed solutions when tanβ is larger than 4, since the tree level mass is directly related to tanβ. However, as we have mentioned before, there is an upper bound on tanβ coming from perturbativity, and combining these two bounds limits the allowed range to a small region.

In scenario II the left-right mixing in the squark sector can be large and we see in Fig. 3 that the lightest stop can be very light, in the 100 GeV region, consistent with the Higgs bounds. The situation is similar in both models, in the MSSM and the BLMSSM. However, in the BLMSSM we find more solutions that correspond to the Higgs mass in the range, 122 GeV $\leq M_h \leq$ 128 GeV, due to the contributions of the new leptons. Notice that the heaviest stop can be as light as 500 GeV in both models. In this scenario we do not find any relevant lower bound on tanβ since it is easier to satisfy the Higgs bounds. See Fig. 4 for the numerical results in the tan$\beta - M_{\tilde{t}_1}$ plane.

V. RADIATIVE HIGGS DECAYS: $h \to \gamma\gamma$ AND $h \to gg$

As it is well known, the excess reported by CMS and ATLAS are in the $\gamma\gamma$ channel, while the other channels are mainly SM-like. Now, knowing the allowed parameter space consistent with a Higgs mass, M_h = 115–128 GeV, we can show the predictions for the radiative Higgs decays.

The Higgs decays at tree level are not modified, but the radiative Higgs decays, $h \to \gamma\gamma$, $h \to gg$, and $h \to Z\gamma$ can be modified due to the existence of new leptons and their superpartners. For the study of the Higgs decay into two

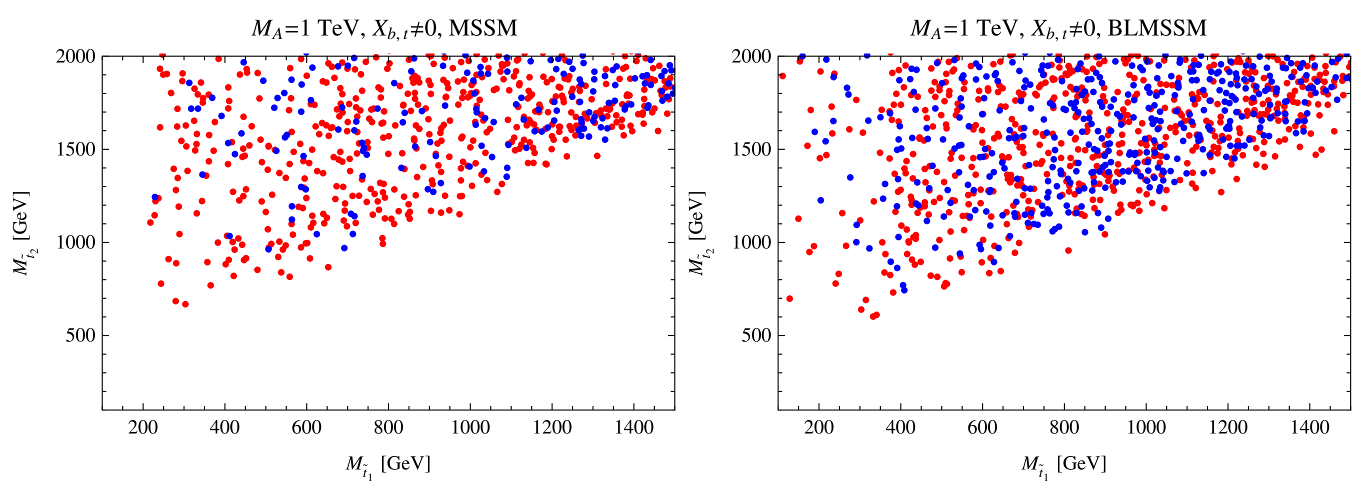

FIG. 3 (color online). Allowed parameter space in the MSSM and BLMSSM in the nonzero mixing scenario $X_t \neq 0$ and $X_b \neq 0$. We use as input parameters $M_{\nu_4} = M_{\nu_5} = 90$ GeV and $M_{e_4} = M_{e_5} = 100$ GeV.

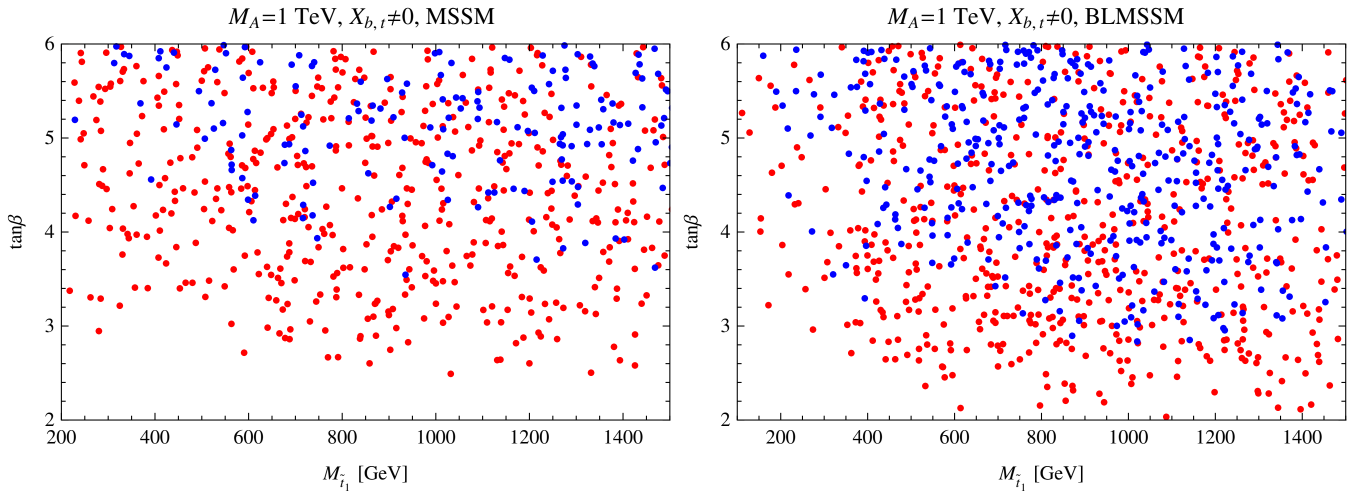

FIG. 4 (color online). Allowed parameter space in the MSSM and BLMSSM in the nonzero mixing scenario $X_t \neq 0$ and $X_b \neq 0$. We use as input parameters $M_{\nu_4} = M_{\nu_5} = 90$ GeV and $M_{e_4} = M_{e_5} = 100$ GeV.

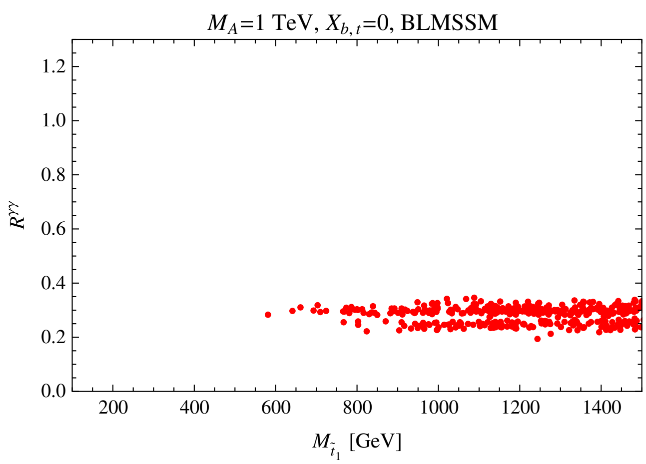

FIG. 5 (color online). Predictions for $R^{\gamma\gamma}$ in scenario I.

photons in the decoupling limit in the MSSM see Ref. [30]. In Fig. 5 we show the predictions for the ratio $R^{\gamma\gamma}$ defined as

$$R^{\gamma\gamma} = \frac{\Gamma(h \to \gamma\gamma)}{\Gamma(h \to \gamma\gamma)_{\rm SM}}, \tag{31}$$

where we have scanned over the ranges mentioned in the previous section and assume zero left-right mixing. Here we show only the predictions in the BLMSSM because in the MSSM one cannot satisfy the Higgs bounds. Notice that the ratio $R^{\gamma\gamma}$ is around 0.3 due to the suppression of the new leptons and their superpartners. In the nonsupersymmetric version of the model this effect was studied in Ref. [31]. In our case the new sleptons further suppress this ratio if they are very light.

In scenario II the situation is quite different because the stops can be very light and the left-right mixing can play a role is the enhancement of the $R^{\gamma\gamma}$ ratio. In Fig. 6 we see

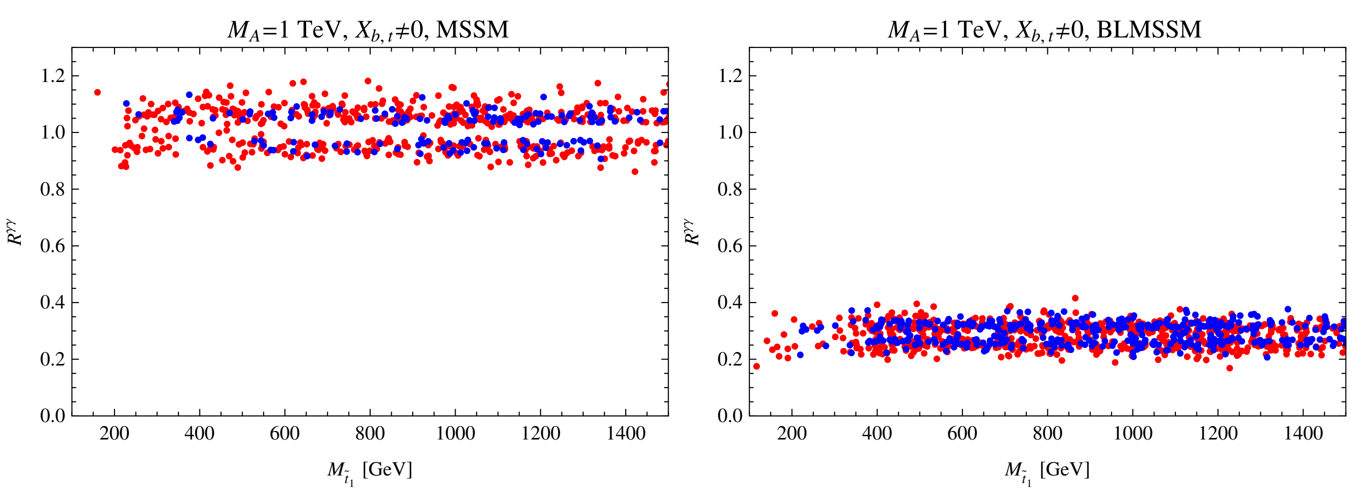

FIG. 6 (color online). Predictions for $R^{\gamma\gamma}$ when $X_t \neq 0$ and $X_b \neq 0$.

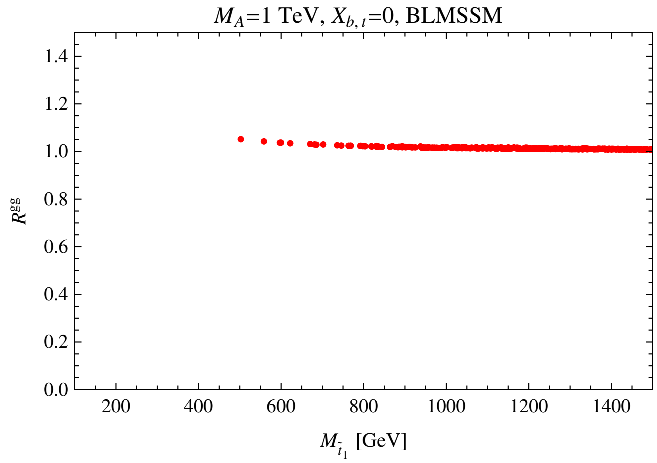

FIG. 7 (color online). Predictions for R^{gg} in scenario I.

that in the MSSM the predictions are SM-like but the ratio can change between 0.85 and 1.2 in the whole parameter space. In the BLMSSM the situation is different since the $R^{\gamma\gamma}$ ratio can be between 0.1 and 0.4. Therefore, one can say that in the BLMMSM one expects a large suppression for the $gg \to h \to \gamma\gamma$ signals. In our opinion, since still the experimental collaborations do not have enough results to claim a discovery, we only take these results as a hint against this model. In order to understand the impact of the SUSY spectrum on the Higgs signals we need to study the radiative decays, $h \to gg$. We define the quantity

$$R^{gg} = \frac{\Gamma(h \to gg)}{\Gamma(h \to gg)_{\rm SM}}, \tag{32}$$

and show the predictions in scenarios I and II in Figs. 7 and 8, respectively. It is easy to understand that in scenario I this ratio is not modified because the stops are heavy. In the second scenario the situation is different because the stops can be light and the left-right mixing can change the sign of the stop contribution. These results are shown in Fig. 8, where we can see that in the MSSM the ratio R^{gg} can be between 0.6 and 1, while in the BLMSSM the range can be 0.2–1.3 when the stop is very light and the left-right mixing is large. It is important to mention that the R^{gg} cannot be too different from the SM because at the moment there are not large excesses in other channels where the Higgs decays into two gauge bosons.

Since the relevant quantity for the experiments is defined as

$$C_{\gamma\gamma} = \frac{\sigma(gg \to h) \times {\rm Br(h \to \gamma\gamma)}}{\sigma(gg \to h)_{\rm SM} \times {\rm Br}(h \to \gamma\gamma)_{\rm SM}} \approx \frac{\Gamma(h \to gg) \times {\rm Br(h \to \gamma\gamma)}}{\Gamma(h \to gg)_{\rm SM} \times {\rm Br(h \to \gamma\gamma)_{SM}}}, \tag{33}$$

where we have used the narrow-width approximation where the cross section is proportional to the Higgs decay width into two gluons, see for example [32], we will use the last part of the above expression to calculate the predictions made by the MSSM and the BLMSSM.

Knowing the results in Figs. 5–8, we can show the predictions for the $C_{\gamma\gamma}$. Since $\gamma\gamma$ and gg ratios are SM-like in the MSSM, in Fig. 10 we see that $C_{\gamma\gamma}$ is SM-like, but it can change between 0.8 and 1.1. In the BLMSSM we just extrapolate the suppression in the $\gamma\gamma$ channel to see that there is a suppression for the signals in this channel. See Figs. 9 and 10 for details.

In summary, we can see that in the context of the BLMMSM one predicts less events in the $gg \to h \to \gamma\gamma$ channel. Therefore, one could rule out this model in the near future if the signals around $M_h \sim 125$ GeV are confirmed by the LHC experiments.

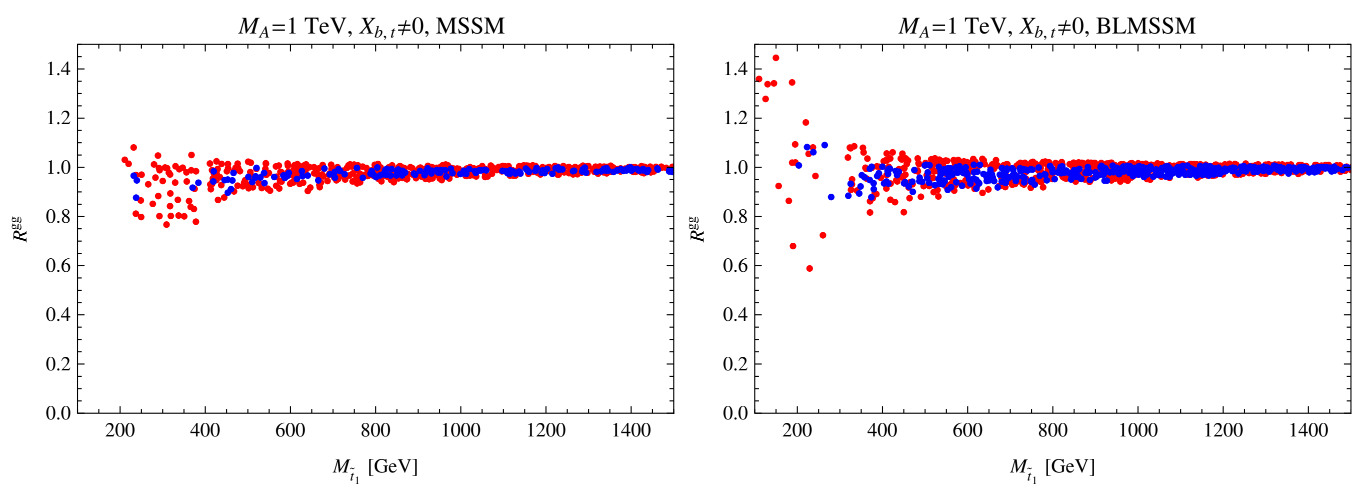

FIG. 8 (color online). Predictions for R^{gg} when $X_t \neq 0$ and $X_b \neq 0$.

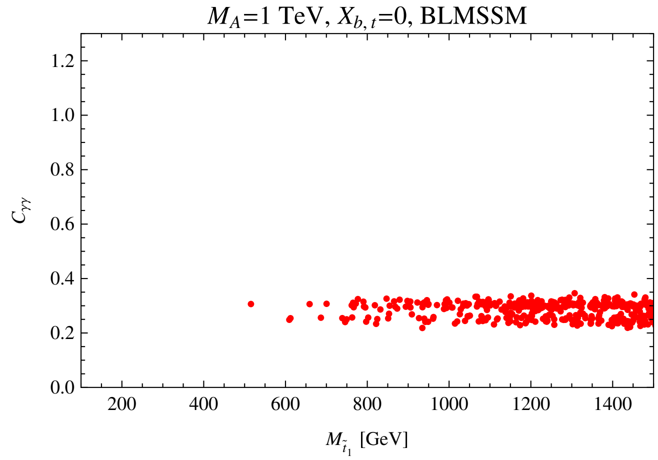

FIG. 9 (color online). Predictions for $C_{\gamma\gamma}$ in scenario I.

VI. EVOLUTION OF THE GAUGE AND YUKAWA COUPLINGS

The evolution of the gauge couplings at one-loop level is given by the well-known expression

$$\frac{1}{\alpha_a(\Lambda_1)} = \frac{1}{\alpha_a(\Lambda_2)} + \frac{b_a}{2\pi} \mathrm{Log}\left(\frac{\Lambda_2}{\Lambda_1}\right), \qquad (34)$$

where $\alpha_a = g_a^2/4\pi$, b_a are the beta functions for the different groups, and Λ_i is a given scale. In order to make the numerical study we will assume that only the new leptons exist below the SUSY scale while the thresholds associated with the new sleptons, new quarks and new squarks are numerically close to the SUSY scale.

The new leptons therefore effect the b_a values of the SM gauge group. They are

$$b_3 = -7, \qquad b_2 = -\frac{15}{6}, \qquad b_1 = \frac{53}{10}, \qquad (35)$$

while above the SUSY scale

$$b_3 = 1, \qquad b_2 = 5, \qquad b_1 = \frac{53}{5}, \qquad (36)$$

$$b_B = N_B(26B_4^2 + \tfrac{80}{3}B_4 + \tfrac{170}{9}), \quad b_L = N_L(8L_4^2 + 24L_4 + 56), \qquad (37)$$

where N_B and N_L are the normalizations for $U(1)_B$ and $U(1)_L$. While it is unclear what these values should be without knowledge of the high scale physics, we will use, for simplicity, $N_B = N_L = \frac{1}{2}$. Also using $B_4 = -1/2$ and $L_4 = -3/2$ we show in Fig. 11 the running of the gauge couplings when $\alpha_B = 0.026$ and $\alpha_L = 0.01$ at the SUSY scale. As one can see from these results, we can keep the unification of the gauge couplings of the MSSM and we can have a simple solution for the unification of the α_L and α_B at the scale 10^{16} GeV. In this way one can imagine a possible unified theory at the high scale. This type of GUT model will be investigated in a future publication.

In order to study the possible existence of a Landau pole we study here the evolution of the Yukawa couplings. See Appendix D for the renormalization group of equations for these couplings. The matching conditions for the Yukawa couplings at the SUSY scale are

$$Y_i = \frac{h_i}{\sin\beta}, \qquad Y_j = \frac{h_j}{\cos\beta}, \qquad i = t, \nu_4, e_5, \qquad j = b, \tau, e_4, \nu_5, \qquad (38)$$

therefore giving a boost to the latter set of Yukawa couplings for $\tan\beta > 1$. In Fig. 12 we show the evolution of the largest Yukawa couplings (Y_t, Y_{e_4}, Y_{ν_5}) for two different scenarios: (a) $m_{\nu_4} = m_{\nu_5} = 90$ GeV and $\tan\beta = 2$, (b) $m_{\nu_4} = m_{\nu_5} = 50$ GeV, $m_{e_4} = m_{e_5} = 100$ GeV and for $\tan\beta = 1.4$. In the first scenario the Landau pole is around 10^7 GeV, while when $\tan\beta = 1.4$ there is a Landau pole at the scale, 10^{14} GeV. In order to show more general results we show in Fig. 13 the isoplot for the scale where we have a Landau pole in the $m_{e_4} - \tan\beta$ plane. It is important to mention that in general the cutoff of theory can be very large. However, since the local baryon number is broken at

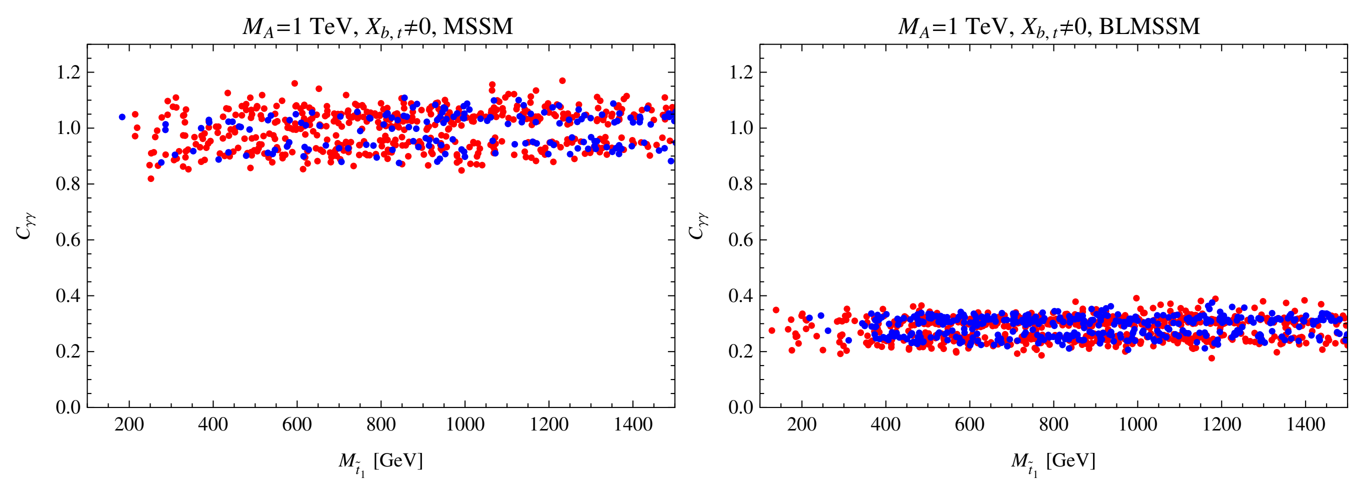

FIG. 10 (color online). Predictions for $C_{\gamma\gamma}$ when $X_t \neq 0$ and $X_b \neq 0$.

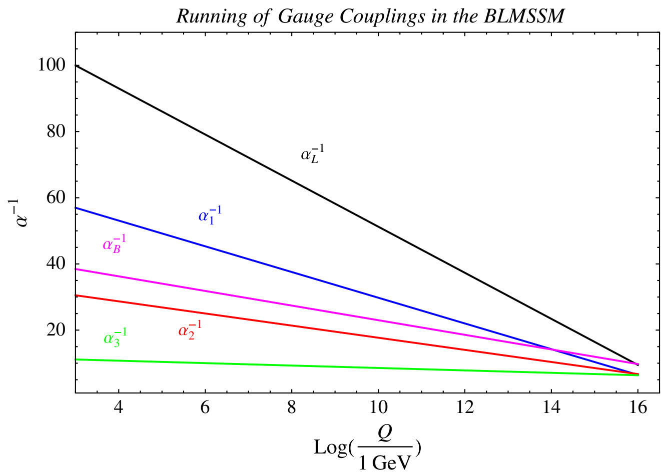

FIG. 11 (color online). Running of the gauge couplings in the BLMSSM assuming $\alpha_B = 0.026$ and $\alpha_L = 0.01$ at the SUSY scale.

the low scale we do not need to assume a large cutoff or the desert in order to satisfy the bounds on the proton decay lifetime.

VII. SUMMARY

We have discussed the main features of a simple extension of the minimal supersymmetric standard model where the baryon and lepton numbers are local symmetries. We refer to this theory as the BLMSSM. In this context we do not need to assume a large desert between the electroweak scale and grand unified scale in order to satisfy the proton decay bounds even if B and L are broken at the low scale. In this context the lepton number is broken in an even number while the baryon number violating operators can change B in one unit. There is no flavor violation at tree level due to absence of mixing between the SM fermion and new families and Landau pole at the low scale. The light Higgs boson mass can be large without assuming a large stop mass and left-right mixing and one could modify the current LHC bounds on the supersymmetric spectrum due to the presence of the baryon number violating interactions.

In Sec. III we discussed the constraints on the λ''_{ijk} from cosmology and the impact of these couplings on the LHC searches for supersymmetric particles. In this case we can have very interesting signals without missing energy. For example, if the stop is the lightest supersymmetric particle one can have signals with displaced vertices and four jets. These are interesting signals and can shed light on the possibility to have light stops in the spectra.

We have investigated in great detail the correlation between the light Higgs mass and the decay of the Higgs boson into two photons following the new results presented by the ATLAS and CMS collaborations. In this theory the new light leptons modify appreciably the predictions of the Higgs decays into two gammas. The constraints on the Higgs mass tell us how light the lightest stop, $M_{\tilde{t}_1}$, can be and since B is broken we can satisfy the collider bounds. We have found that in the context of the BLMMSM one predicts less events in the $gg \to h \to \gamma\gamma$ channel. Therefore, one could rule out this model in the near future if the signals around, $M_h \sim 125$ GeV, are confirmed by the LHC experiments.

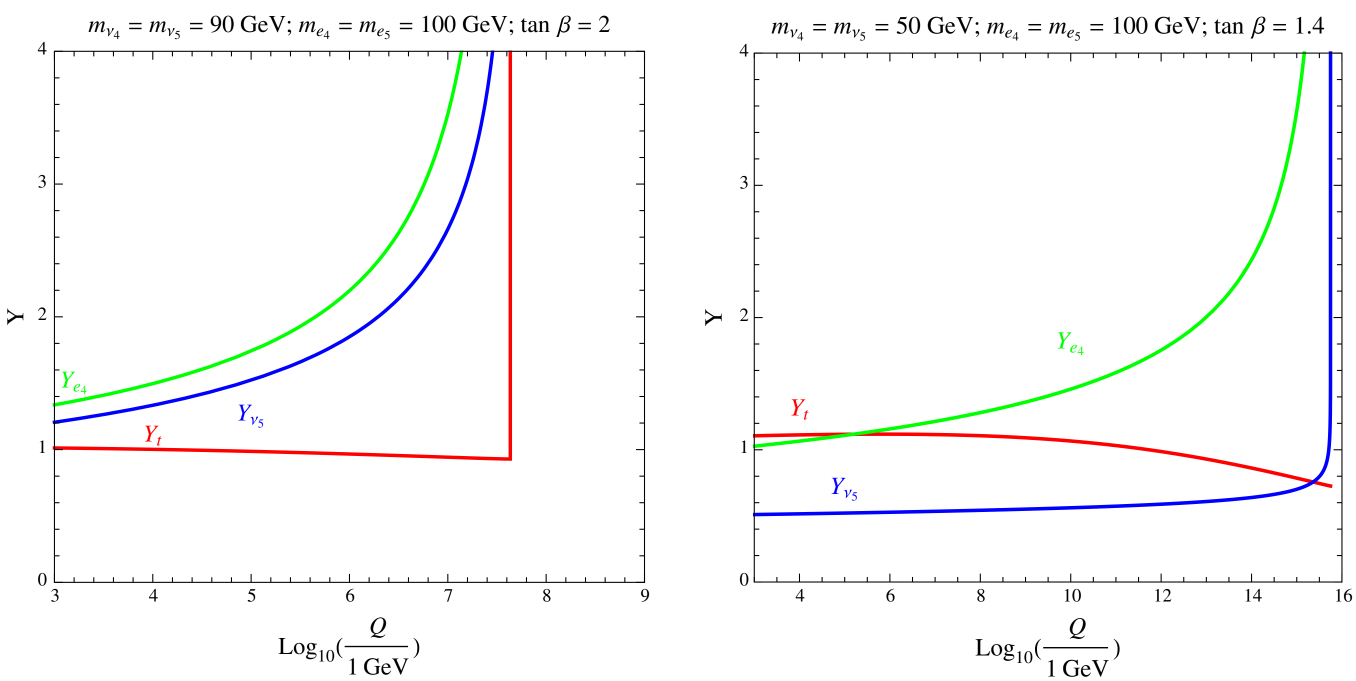

FIG. 12 (color online). Yukawa coupling running in the BLMSSM for Y_t, Y_{e_4}, and Y_{ν_5} above the SUSY scale for $m_{\nu_4} = m_{\nu_5} =$ 90(50) GeV and $m_{e_4} = m_{e_5} = 100$ GeV and for tan$\beta = 2(1.4)$ with gauge couplings as in Fig. 11.

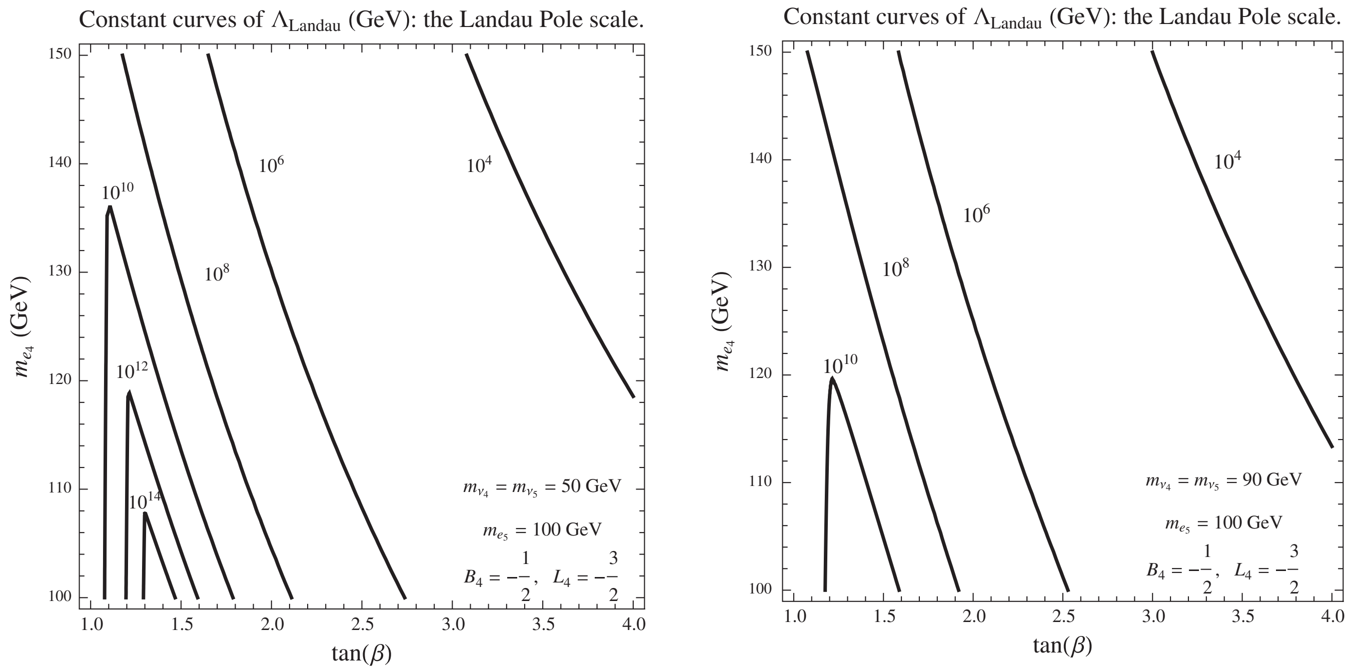

FIG. 13. Isoplot for the scale where one has a Landau pole in the $m_{e_4} - \tan\beta$ plane.

In this theory the fields X and $\bar{X}$ (or their superpartners) can be cold dark matter candidates if they are the lightest fields with baryon number and do not get a vacuum expectation value. This is true even when R-parity is broken in this theory. This is an interesting result that we will investigate in a future publication. See Ref. [5] for the study of this dark matter candidate in a nonsupersymmetric version of the model.

The running of the Yukawa couplings were studied in order to understand the possible cutoff of the theory. We have found that for small values of $\tan\beta$ the cutoff of the theory can be very large. It is important to mention that since the baryon and lepton numbers are broken at the low scale, there is no need to have a large cutoff. In summary, we could say that the BLMSSM is a consistent theory where one could expect a light stop-sbottom spectrum in agreement with all experiments and that predicts new light leptons. The collider signals of this theory will be investigated in a future publication.

ACKNOWLEDGMENTS

We would like to thank Mark B. Wise for discussions and many interesting comments. The work of P. F. P. has been supported by the James Arthur foundation, CCPP, New York University. The work of J. M. A. and B. F. was supported in part by the U.S. Department of Energy under Contract No. DE-FG02-92ER40701.

APPENDIX A: PARTICLE CONTENT

Table I gives the superfields present in the BLMSSM.

TABLE I. The index $i = 1, 2, 3$.

Superfields	$SU(3)_C$	$SU(2)_L$	$U(1)_Y$	$U(1)_B$	$U(1)_L$
$\hat{Q}_i$	3	2	1/6	1/3	0
$\hat{u}_i^c$	$\bar{3}$	1	$-2/3$	$-1/3$	0
$\hat{d}_i^c$	$\bar{3}$	1	1/3	$-1/3$	0
$\hat{L}_i$	1	2	$-1/2$	0	1
$\hat{e}_i^c$	1	1	1	0	-1
$\hat{\nu}_i^c$	1	1	0	0	-1
$\hat{Q}_4$	3	2	1/6	B_4	0
$\hat{u}_4^c$	$\bar{3}$	1	$-2/3$	$-B_4$	0
$\hat{d}_4^c$	$\bar{3}$	1	1/3	$-B_4$	0
$\hat{L}_4$	1	2	$-1/2$	0	L_4
$\hat{e}_4^c$	1	1	1	0	$-L_4$
$\hat{\nu}_4^c$	1	1	0	0	$-L_4$
$\hat{Q}_5^c$	$\bar{3}$	2	$-1/6$	$-1 - B_4$	0
$\hat{u}_5$	3	1	2/3	$1 + B_4$	0
$\hat{d}_5$	3	1	$-1/3$	$1 + B_4$	0
$\hat{L}_5^c$	1	2	1/2	0	$-3 - L_4$
$\hat{e}_5$	1	1	-1	0	$3 + L_4$
$\hat{\nu}_5$	1	1	0	0	$3 + L_4$
$\hat{H}_u$	1	2	1/2	0	0
$\hat{H}_d$	1	2	$-1/2$	0	0
$\hat{S}_B$	1	1	0	1	0
$\hat{\bar{S}}_B$	1	1	0	-1	0
$\hat{S}_L$	1	1	0	0	-2
$\hat{\bar{S}}_L$	1	1	0	0	2
$\hat{X}$	1	1	0	$2/3 + B_4$	0
$\hat{\bar{X}}$	1	1	0	$-2/3 - B_4$	0

APPENDIX B: SFERMION MASSES

The sbottom mass matrix is defined by

$$\mathcal{M}^2_{\tilde{b}} = \begin{pmatrix} M_b^2 + M^2_{\tilde{Q}_3} - \left(\frac{1}{2} - \frac{1}{3}\sin^2\theta_W\right) M_Z^2 \cos 2\beta + \frac{1}{3} D_B & M_b X_b \\ M_b X_b & M_b^2 + M^2_{\tilde{d}_3^c} - \frac{1}{3}\sin^2\theta_W M_Z^2 \cos 2\beta - \frac{1}{3} D_B \end{pmatrix}, \tag{B1}$$

where $M^2_{\tilde{d}_3^c}$ is a soft mass, $D_B = \frac{1}{2} M^2_{Z_B} \cos 2\beta_B$, and $X_b = A_b - \mu \tan\beta$. The mass matrix for the new sleptons is given by

$$\mathcal{M}^2_{\tilde{e}_4} = \begin{pmatrix} M_{e_4}^2 + M^2_{\tilde{L}_4} - \left(\frac{1}{2} - \sin^2\theta_W\right) M_Z^2 \cos 2\beta + L_4 D_L & M_{e_4} X_{e_4} \\ M_{e_4} X_{e_4} & M_{e_4}^2 + M^2_{\tilde{e}_4^c} - \sin^2\theta_W M_Z^2 \cos 2\beta - L_4 D_L \end{pmatrix}, \tag{B2}$$

where $M^2_{\tilde{L}_4}$ and $M^2_{\tilde{e}_4^c}$ are soft masses, $D_L = -\frac{1}{4} M^2_{Z_L} \cos 2\beta_L$ and $X_{e_4} = A_{e_4} - \mu \tan\beta$. The mass matrix for the fourth generation heavy neutrino is given by

$$\mathcal{M}^2_{\tilde{\nu}_4} = \begin{pmatrix} M_{\nu_4}^2 + M^2_{\tilde{L}_4} + \frac{1}{2} M_Z^2 \cos 2\beta + L_4 D_L & M_{\nu_4} X_{\nu_4} \\ M_{\nu_4} X_{\nu_4} & M_{\nu_4}^2 + M^2_{\tilde{\nu}_4^c} - L_4 D_L \end{pmatrix}, \tag{B3}$$

where $X_{\nu_4} = A_{\nu_4} - \mu \cot\beta$. In the case of the leptons of the fifth generation the mass matrices read as

$$\mathcal{M}^2_{\tilde{e}_5} = \begin{pmatrix} M_{e_5}^2 + M^2_{\tilde{L}_5^c} + \left(\frac{1}{2} - \sin^2\theta_W\right) M_Z^2 \cos 2\beta + L_5 D_L & M_{e_5} X_{e_5} \\ M_{e_5} X_{e_5} & M_{e_5}^2 + M^2_{\tilde{e}_5} + \sin^2\theta_W M_Z^2 \cos 2\beta - L_5 D_L \end{pmatrix}, \tag{B4}$$

with $X_{e_5} = A_{e_5} - \mu \tan\beta$ and $L_5 = -(L_4 + 3)$. Notice that in order to have the mass matrices for squarks in the MSSM one has to set $D_B = 0$. Knowing the sfermion spectrum we are ready to discuss the predictions for the Higgs mass.

APPENDIX C: CONTRIBUTIONS TO $h \to \gamma\gamma$ AND $h \to gg$

The formulas presented in this section were adopted from Ref. [30]. The two-photon decay width of a CP-even Higgs particle h can be written as

$$\Gamma(h \to \gamma\gamma) = \frac{G_F \alpha_{\rm EW}^2 M_h^3}{128\sqrt{2}\pi^3} \left| \sum_i A_i(\tau_i) \right|^2, \tag{C1}$$

where $\tau_i = M_\Phi^2/(4m_i^2)$ with m_i being the mass of the loop particle. The amplitudes are given by

$$A_W(\tau_W) = g_{\Phi WW} F_1(\tau_W), \tag{C2}$$

$$A_f(\tau_f) = N_c Q_f^2 g_{\Phi ff} F_{1/2}(\tau_f), \tag{C3}$$

$$A_{H^\pm}(\tau_{H^\pm}) = g_{\Phi H^+ H^-} \frac{M_W^2}{M_{H^\pm}^2} F_0(\tau_{H^\pm}), \tag{C4}$$

$$A_{\chi_i}(\tau_{\chi_i}) = g_{\Phi \chi_i^+ \chi_i^-} \frac{M_W}{m_{\chi_i}} F_{1/2}(\tau_{\chi_i}), \tag{C5}$$

$$A_{\tilde{f}_i}(\tau_{\tilde{f}_i}) = N_c Q_f^2 g_{\Phi \tilde{f}_i \tilde{f}_i} \frac{M_Z^2}{m^2_{\tilde{f}_i}} F_0(\tau_{\tilde{f}_i}), \tag{C6}$$

where N_c is the color factor and Q_f is the electric charge of the fermion/sfermion in units of the proton charge. The functions F are given by

$$F_0(\tau) = \frac{\tau - f(\tau)}{\tau^2}, \tag{C7}$$

$$F_{1/2}(\tau) = -\frac{2[\tau + (\tau - 1) f(\tau)]}{\tau^2}, \tag{C8}$$

$$F_1(\tau) = \frac{2\tau^2 + 3\tau + 3(2\tau - 1) f(\tau)}{\tau^2}, \tag{C9}$$

where

$$f(\tau) = \begin{cases} \arcsin^2\sqrt{\tau} & \tau \le 1, \\ -\frac{1}{4}\left[\log\left(\frac{1+\sqrt{1-1/\tau}}{1-\sqrt{1-1/\tau}}\right) - i\pi\right]^2 & \tau > 1. \end{cases} \tag{C10}$$

The mixing angle α, which we use in subsequent formulas, is expressed by

$$\alpha = \frac{1}{2} \arctan\left[\frac{2(\mathcal{M}^2_{\rm even})_{12}}{(\mathcal{M}^2_{\rm even})_{11} - (\mathcal{M}^2_{\rm even})_{22}}\right], \quad \alpha \in \left(-\frac{\pi}{2}, 0\right). \tag{C11}$$

In the decoupling limit ($M_A^2 \gg M_Z^2$) we obtain $\alpha \to \beta - \pi/2$. Values of MSSM couplings in formulas (C2) are as follows:

(a) W boson loop ($g_{H^0 WW} = 1$ in SM),

$$g_{hWW} = \sin(\beta - \alpha). \tag{C12}$$

(b) Fermion loops ($g_{H^0uu} = g_{H^0dd} = 1$ in SM),

$$g_{huu} = \frac{\cos\alpha}{\sin\beta}, \qquad g_{hdd} = -\frac{\sin\alpha}{\cos\beta}. \tag{C13}$$

(c) Charged Higgs loops (negligible in the decoupling regime),

$$g_{hH^+H^-} = \sin(\beta - \alpha) + \frac{\cos(2\beta)\sin(\alpha + \beta)}{2\cos^2\theta_W} + \frac{\epsilon\cos\alpha\cos^2\beta}{2\cos^2\theta_W M_Z^2 \sin\beta}. \tag{C14}$$

(d) Top squark loops

$$g_{h\tilde{t}_1\tilde{t}_1} = -\frac{1}{2}\sin(\alpha+\beta)\left[\cos^2\theta_t - \frac{4}{3}\sin^2\theta_W\cos2\theta_t\right] + \frac{\cos\alpha}{\sin\beta}\frac{m_t^2}{M_Z^2} + \frac{m_t\sin2\theta_t}{2M_Z^2}\left[\frac{\cos\alpha}{\sin\beta}A_t + \frac{\sin\alpha}{\sin\beta}\mu\right], \tag{C15}$$

$$g_{h\tilde{t}_2\tilde{t}_2} = -\frac{1}{2}\sin(\alpha+\beta)\left[\sin^2\theta_t + \frac{4}{3}\sin^2\theta_W\cos2\theta_t\right] + \frac{\cos\alpha}{\sin\beta}\frac{m_t^2}{M_Z^2} - \frac{m_t\sin2\theta_t}{2M_Z^2}\left[\frac{\cos\alpha}{\sin\beta}A_t + \frac{\sin\alpha}{\sin\beta}\mu\right], \tag{C16}$$

where

$$\sin2\theta_t = \frac{2m_tX_t}{M_{\tilde{t}_1}^2 - M_{\tilde{t}_2}^2}. \tag{C17}$$

(e) Bottom squark loops

$$g_{h\tilde{b}_1\tilde{b}_1} = \frac{1}{2}\sin(\alpha+\beta)\left[\cos^2\theta_b - \frac{2}{3}\sin^2\theta_W\cos2\theta_b\right] - \frac{\sin\alpha}{\cos\beta}\frac{m_b^2}{M_Z^2} + \frac{m_b\sin2\theta_b}{2M_Z^2}\left[\frac{\sin\alpha}{\cos\beta}A_b + \frac{\cos\alpha}{\cos\beta}\mu\right], \tag{C18}$$

$$g_{h\tilde{b}_2\tilde{b}_2} = \frac{1}{2}\sin(\alpha+\beta)\left[\sin^2\theta_b + \frac{2}{3}\sin^2\theta_W\cos2\theta_b\right] - \frac{\sin\alpha}{\cos\beta}\frac{m_b^2}{M_Z^2} - \frac{m_b\sin2\theta_b}{2M_Z^2}\left[\frac{\sin\alpha}{\cos\beta}A_b + \frac{\cos\alpha}{\cos\beta}\mu\right], \tag{C19}$$

where

$$\sin2\theta_b = \frac{2m_bX_b}{M_{\tilde{b}_1}^2 - M_{\tilde{b}_2}^2}. \tag{C20}$$

(f) Fourth family selectron loops

$$g_{h\tilde{e}_4^1\tilde{e}_4^1} = \frac{1}{2}\sin(\alpha+\beta)[\cos^2\theta_{e_4} - 2\sin^2\theta_W\cos2\theta_{e_4}] - \frac{\sin\alpha}{\cos\beta}\frac{m_{e_4}^2}{M_Z^2} + \frac{m_{e_4}\sin2\theta_{e_4}}{2M_Z^2}\left[\frac{\sin\alpha}{\cos\beta}A_{e_4} + \frac{\cos\alpha}{\cos\beta}\mu\right], \tag{C21}$$

$$g_{h\tilde{e}_4^2\tilde{e}_4^2} = \frac{1}{2}\sin(\alpha+\beta)[\sin^2\theta_{e_4} + 2\sin^2\theta_W\cos2\theta_{e_4}] - \frac{\sin\alpha}{\cos\beta}\frac{m_{e_4}^2}{M_Z^2} - \frac{m_{e_4}\sin2\theta_{e_4}}{2M_Z^2}\left[\frac{\sin\alpha}{\cos\beta}A_{e_4} + \frac{\cos\alpha}{\cos\beta}\mu\right], \tag{C22}$$

where

$$\sin2\theta_{e_4} = \frac{2m_{e_4}X_{e_4}}{M_{\tilde{e}_4^1}^2 - M_{\tilde{e}_4^2}^2}. \tag{C23}$$

(g) Fifth family selectron loops

$$g_{h\tilde{e}_5^1\tilde{e}_5^1} = -\frac{1}{2}\sin(\alpha+\beta)[\cos^2\theta_{e_5} - 2\sin^2\theta_W\cos2\theta_{e_5}] + \frac{\cos\alpha}{\sin\beta}\frac{m_{e_5}^2}{M_Z^2} + \frac{m_{e_5}\sin2\theta_{e_5}}{2M_Z^2}\left[\frac{\cos\alpha}{\sin\beta}A_{e_5} + \frac{\sin\alpha}{\sin\beta}\mu\right], \tag{C24}$$

$$g_{h\tilde{e}_5^2\tilde{e}_5^2} = -\frac{1}{2}\sin(\alpha+\beta)[\sin^2\theta_{e_5} + 2\sin^2\theta_W\cos2\theta_{e_5}] + \frac{\cos\alpha}{\sin\beta}\frac{m_{e_5}^2}{M_Z^2} - \frac{m_{e_5}\sin2\theta_{e_5}}{2M_Z^2}\left[\frac{\cos\alpha}{\sin\beta}A_{e_5} + \frac{\sin\alpha}{\sin\beta}\mu\right], \tag{C25}$$

where

$$\sin2\theta_{e_5} = \frac{2m_{e_5}X_{e_5}}{M_{\tilde{e}_5^1}^2 - M_{\tilde{e}_5^2}^2}. \tag{C26}$$

(h) Chargino loops

$$g_{h\chi_1^+\chi_1^-} = \sqrt{2}(-\cos\alpha\cos\theta^+\sin\theta^- + \sin\alpha\sin\theta^+\cos\theta^-), \tag{C27}$$

$$g_{h\chi_2^+\chi_2^-} = -\varepsilon\sqrt{2}(-\cos\alpha\cos\theta^-\sin\theta^+ + \sin\alpha\sin\theta^-\cos\theta^+), \tag{C28}$$

where M_2 is the gaugino mass parameter, the function $\varepsilon = \mathrm{sign}(\mu M_2 - M_W^2\sin 2\beta)$, and $\theta^\pm$ can be determined from,

$$\tan 2\theta^+ = \frac{2\sqrt{2}M_W(M_2\cos\beta + \mu\sin\beta)}{M_2^2 - \mu^2 - 2M_W^2\cos 2\beta}, \tag{C29}$$

$$\tan 2\theta^- = \frac{2\sqrt{2}M_W(M_2\sin\beta + \mu\cos\beta)}{M_2^2 - \mu^2 + 2M_W^2\cos 2\beta}. \tag{C30}$$

Chargino masses

$$m_{\chi_{1,2}}^2 = \frac{1}{2}[M_2^2 + \mu^2 + 2M_W^2 \mp \sqrt{(M_2^2 - \mu^2)^2 + 4M_W^4\cos^2 2\beta + 4M_W^2(M_2^2 + \mu^2 + 2M_2\mu\sin 2\beta)}]. \tag{C31}$$

The formula below was adopted from Ref. [33]. The two-gluon decay width of a CP-even Higgs particle h is given by

$$\Gamma(h\to gg) = \frac{9G_F\alpha_s^2 M_h^3}{576\sqrt{2}\pi^3}\left|\sum_q A_q(\tau_q) + \sum_i A_{\tilde{f}_i}(\tau_{\tilde{f}_i})\right|^2, \tag{C32}$$

where $\tau_i = M_\Phi^2/(4m_i^2)$ with m_i being the mass of the loop particle and

$$A_q(\tau_q) = g_{hqq}F_{1/2}(\tau_q). \tag{C33}$$

Therefore, it is expressed in terms of quantities we already know how to calculate from the $h\to\gamma\gamma$ case.

APPENDIX D: RGES FOR THE YUKAWA COUPLINGS

The RGEs in the Yukawa sector below the SUSY scale are modified by the new leptons. Ignoring the lepton and baryon number gauge contributions that are small below the SUSY scale, the Yukawa RGEs below the SUSY scale are

$$16\pi^2\frac{dh_t}{dt} = h_t\left[\frac{9}{2}h_t^2 + \frac{3}{2}h_b^2 + h_\tau^2 + h_{e_4}^2 + h_{e_5}^2 + h_{\nu_4}^2 + h_{\nu_5}^2 - 4\pi\left(\frac{17}{20}\alpha_1 + \frac{9}{4}\alpha_2 + 8\alpha_3\right)\right], \tag{D1}$$

$$16\pi^2\frac{dh_b}{dt} = h_b\left[\frac{9}{2}h_b^2 + \frac{3}{2}h_t^2 + h_\tau^2 + h_{e_4}^2 + h_{e_5}^2 + h_{\nu_4}^2 + h_{\nu_5}^2 - 4\pi\left(\frac{1}{4}\alpha_1 + \frac{9}{4}\alpha_2 + 8\alpha_3\right)\right], \tag{D2}$$

$$16\pi^2\frac{dh_\tau}{dt} = h_\tau\left[\frac{5}{2}h_\tau^2 + 3h_b^2 + 3h_t^2 + h_{e_4}^2 + h_{e_5}^2 + h_{\nu_4}^2 + h_{\nu_5}^2 - 4\pi\left(\frac{9}{4}\alpha_1 + \frac{9}{4}\alpha_2\right)\right], \tag{D3}$$

$$16\pi^2\frac{dh_{\nu_4}}{dt} = h_{\nu_4}\left[\frac{5}{2}h_{\nu_4}^2 - \frac{1}{2}h_{e_4}^2 + 3h_b^2 + 3h_t^2 + h_\tau^2 + h_{e_5}^2 + h_{\nu_5}^2 - 4\pi\left(\frac{3}{4}\alpha_1 + \frac{9}{4}\alpha_2\right)\right], \tag{D4}$$

$$16\pi^2\frac{dh_{e_4}}{dt} = h_{e_4}\left[\frac{5}{2}h_{e_4}^2 - \frac{1}{2}h_{\nu_4}^2 + 3h_b^2 + 3h_t^2 + h_\tau^2 + h_{e_5}^2 + h_{\nu_5}^2 - 4\pi\left(\frac{9}{4}\alpha_1 + \frac{9}{4}\alpha_2\right)\right], \tag{D5}$$

$$16\pi^2\frac{dh_{\nu_5}}{dt} = h_{\nu_5}\left[\frac{5}{2}h_{\nu_5}^2 - \frac{1}{2}h_{e_5}^2 + 3h_b^2 + 3h_t^2 + h_\tau^2 + h_{e_4}^2 + h_{\nu_4}^2 - 4\pi\left(\frac{3}{4}\alpha_1 + \frac{9}{4}\alpha_2\right)\right], \tag{D6}$$

$$16\pi^2\frac{dh_{e_5}}{dt} = h_{e_5}\left[\frac{5}{2}h_{e_5}^2 - \frac{1}{2}h_{\nu_5}^2 + 3h_b^2 + 3h_t^2 + h_\tau^2 + h_{e_4}^2 + h_{\nu_4}^2 - 4\pi\left(\frac{9}{4}\alpha_1 + \frac{9}{4}\alpha_2\right)\right]. \tag{D7}$$

It has been assumed throughout this paper that the Higgs contribution to the masses of the new quarks is negligible translating into small Yukawa couplings that will not greatly affect the running of other Yukawa couplings. They are therefore neglected in the following Yukawa RGEs above the SUSY scale:

$$16\pi^2 \frac{dY_t}{dt} = Y_t\left[6Y_t^2 + Y_b^2 + Y_{\nu_4}^2 + Y_{e_5}^2 - 4\pi\left(\frac{13}{15}\alpha_1 + 3\alpha_2 + \frac{16}{3}\alpha_3 + \frac{4}{9}N_B\alpha_B\right)\right], \tag{D8}$$

$$16\pi^2 \frac{dY_b}{dt} = Y_b\left[6Y_b^2 + Y_t^2 + Y_\tau^2 + Y_{e_4}^2 + Y_{\nu_5}^2 - 4\pi\left(\frac{7}{15}\alpha_1 + 3\alpha_2 + \frac{16}{3}\alpha_3 + \frac{4}{9}N_B\alpha_B\right)\right], \tag{D9}$$

$$16\pi^2 \frac{dY_\tau}{dt} = Y_\tau\left[4Y_\tau^2 + 3Y_b^2 + Y_{e_4}^2 + Y_{\nu_5}^2 - 4\pi\left(\frac{9}{5}\alpha_1 + 3\alpha_2 + 4N_L\alpha_L\right)\right], \tag{D10}$$

$$16\pi^2 \frac{dY_{e_4}}{dt} = Y_{e_4}\left[4Y_{e_4}^2 + 3Y_b^2 + Y_\tau^2 + Y_{\nu_4}^2 + Y_{\nu_5}^2 - 4\pi\left(\frac{9}{5}\alpha_1 + 3\alpha_2 + 4L_4^2N_L\alpha_L\right)\right], \tag{D11}$$

$$16\pi^2 \frac{dY_{\nu_4}}{dt} = Y_{\nu_4}\left[4Y_{\nu_4}^2 + 3Y_t^2 + Y_{e_4}^2 + Y_{e_5}^2 - 4\pi\left(\frac{3}{5}\alpha_1 + 3\alpha_2 + 4L_4^2N_L\alpha_L\right)\right], \tag{D12}$$

$$16\pi^2 \frac{dY_{e_5}}{dt} = Y_{e_5}\left[4Y_{e_5}^2 + 3Y_t^2 + Y_{\nu_4}^2 + Y_{\nu_5}^2 - 4\pi\left(\frac{9}{5}\alpha_1 + 3\alpha_2 + 4N_L(L_4+3)^2\alpha_L\right)\right], \tag{D13}$$

$$16\pi^2 \frac{dY_{\nu_5}}{dt} = Y_{\nu_5}\left[4Y_{\nu_5}^2 + 3Y_b^2 + Y_\tau^2 + Y_{e_4}^2 + Y_{e_5}^2 - 4\pi\left(\frac{3}{5}\alpha_1 + 3\alpha_2 + 4N_L(L_4+3)^2\alpha_L\right)\right]. \tag{D14}$$

We remind the reader that N_B and N_L are the normalization factors for $U(1)_B$ and $U(1)_L$ and have both been chosen to be half for the numerical work in this paper for simplicity.

[1] Supersymmetry Searches at CMS, http://cms.web.cern.ch/org/cms-papers-and-results.
[2] Supersymmetry Searches at ATLAS, https://twiki.cern.ch/twiki/bin/view/AtlasPublic/SupersymmetryPublicResults.
[3] P. Fileviez Pérez and M. B. Wise, J. High Energy Phys. 08 (2011) 068.
[4] P. Fileviez Perez and M. B. Wise, Phys. Rev. D **82**, 011901 (2010); **82**, 079901(E) (2010). See also P. Fileviez Perez and M. B. Wise, Phys. Rev. D **84**, 055015 (2011).
[5] T. R. Dulaney, P. Fileviez Perez, and M. B. Wise, Phys. Rev. D **83**, 023520 (2011).
[6] J. Alitti *et al.* (UA2 Collaboration), Nucl. Phys. **B400**, 3 (1993).
[7] S. Chatrchyan *et al.* (CMS Collaboration), arXiv:1204.2488.
[8] P. Langacker, arXiv:0911.4294.
[9] B. A. Campbell, S. Davidson, J. R. Ellis, and K. A. Olive, Phys. Lett. B **256**, 484 (1991).
[10] B. A. Campbell, S. Davidson, J. R. Ellis, and K. A. Olive, Astropart. Phys. **1**, 77 (1992).
[11] W. Fischler, G. F. Giudice, R. G. Leigh, and S. Paban, Phys. Lett. B **258**, 45 (1991).
[12] H. K. Dreiner and G. G. Ross, Nucl. Phys. **B410**, 188 (1993).
[13] G. R. Farrar and P. Fayet, Phys. Lett. **76B**, 575 (1978).
[14] J. H. Kuhn and S. Ono, Phys. Lett. **142B**, 436 (1984).
[15] J. T. Goldman and H. Haber, Physica D (Amsterdam) **15**, 181 (1985).
[16] I. I. Y. Bigi, V. S. Fadin, and V. A. Khoze, Nucl. Phys. **B377**, 461 (1992).
[17] E. Chikovani, V. Kartvelishvili, R. Shanidze, and G. Shaw, Phys. Rev. D **53**, 6653 (1996).
[18] K. Cheung, W.-Y. Keung, Phys. Rev. D **71**, 015015 (2005).
[19] M. Drees and X. Tata, Phys. Lett. B **252**, 695 (1990).
[20] J. L. Feng and T. Moroi, Phys. Rev. D **58**, 035001 (1998).
[21] Michael D. Litos, Ph.D. thesis, Boston University, 2010.
[22] J. L. Goity and M. Sher, Phys. Lett. B **346**, 69 (1995); **385**, 500(E) (1996).
[23] ATLAS Collaboration, Phys. Rev. Lett. **108**, 111803 (2012).
[24] ATLAS Collaboration, Phys. Lett. B **710**, 49 (2012).
[25] CMS Collaboration, Phys. Lett. B **710**, 26 (2012).
[26] CMS Collaboration, Phys. Lett. B **710**, 403 (2012).
[27] CMS physics analysis, https://cdsweb.cern.ch/record/1429928/files/HIG-12-008-pas.pdf.
[28] S. Heinemeyer, W. Hollik, and G. Weiglein, Comput. Phys. Commun. **124**, 76 (2000); Eur. Phys. J. C **9**, 343 (1999); G. Degrassi, S. Heinemeyer, W. Hollik, P. Slavich, and G. Weiglein, Eur. Phys. J. C **28**, 133 (2003); M. Frank,

T. Hahn, S. Heinemeyer, W. Hollik, H. Rzehak, and G. Weiglein, J. High Energy Phys. 02 (**2007**) 047.
[29] P. Fileviez Perez, Phys. Lett. B **711**, 353 (2012).
[30] A. Djouadi, V. Driesen, W. Hollik, and J. I. Illana, Eur. Phys. J. C **1**, 149 (1998).
[31] K. Ishiwata and M. B. Wise, Phys. Rev. D **84**, 055025 (2011).
[32] M. Spira, Fortschr. Phys. **46**, 203 (1998).
[33] A. Djouadi, Phys. Rep. **457**, 1 (2008).